 CMC, vol.15, no.2, pp.129-151, 2010

Computational Homology, Connectedness, and Structure-Property Relations

Dustin D. Gerrard[1], David T. Fullwood[1], Denise M. Halverson[2] and Stephen R. Niezgoda[3]

Abstract: The effective properties of composite materials are often strongly related to the connectivity of the material components. Many structure metrics, and related homogenization theories, do not effectively account for this connectivity. In this paper, relationships between the topology, represented via homology theory, and the effective elastic response of composite plates is investigated. The study is presented in the context of popular structure metrics such as percolation theory and correlation functions.

Keywords: Homology, Topology, Stiffness, Microstructure.

1 Introduction

Understanding the linkages between a material's internal structure, or microstructure, and its properties is the cornerstone of the field of materials science and engineering. The microstructure features that contribute to effective properties or macroscale response span multiple length scales from the atomic to the macroscale. The understanding that the effects from features at these disparate length scales are strongly coupled drives the current efforts in the field of multi-scale and multi-physics modeling [Curtin and Miller (2003), Phillips (2001), Rudd and Broughton (2000), Zbib and Diaz de la Rubia (2002)]. For the foreseeable future multi-scale models that explicitly model the microstructure across all length scales are computationally impossible, and we must rely on homogenization or averaging techniques to pass effective local properties from the lower length scales up the chain. In a very real sense the grand challenge in multi-scale modeling is to develop computationally efficient homogenization relationships based on the observed microstructure.

Many properties of interest are strongly dependent on the connectivity present in

[1] Department of Mechanical Engineering, Brigham Young University, Provo UT
[2] Department of Mathematics, Brigham Young University, Provo UT
[3] Department of Materials Science and Engineering, Drexel University., Philadelphia, PA

the microstructure; conductivity being the trivial example. For high contrast composites and porous solids it is natural to assume that differences in connectivity of the stiffer or stronger phase will have a large affect on the effective properties of the material. Previously, percolation theory [Arbabi and Sahimi (1993), Bergman (1986), Kantor and Webman (1984), Roberts and Garboczi (2002)], statistical metrics such as the 2-point correlations, and the lineal path function [Beran, Mason, Adams and Olsen (1996), Ju and Chen (1994), Kumar, Briant and Curtin (2006), Sankaran and Zabaras (2006), Torquato (2002)], and simple topological measures such as the Euler characteristic [Mecke (1996), Mecke and Sofonea (1997), Mendoza, Thornton, Savin and Voorhees (2006), Steele (1972)] have all been employed to tease out these relationships. Characterization of networks and connectivity by the homology groups from algebraic topology has been utilized in several other fields (for examples, see [Ghrist and Muhammad (2005), Goubault and Jensen (1992), Mezey (1985)] among others) but has only recently been explored in the field of materials science [Gameiro, Mischaikow and Wanner (2005), Wanner, Fuller Jr and Saylor (2010)].

In this study we seek to establish a relationship between the effective elastic properties of a heterogeneous microstructure and its associated homology group[1]. The main case study will involve a two-phase heterogeneous plate with a high contrast of elastic stiffness between the phases. A recent study has identified a weak correlation between the Betti numbers describing the homology group of a heterogeneous material, and elastic properties .[Adams (Submitted)]. This paper presents a more comprehensive study of the relationships, considers relationships between homology and percolation metrics, and investigates potential improvements in the definition of homology-type metrics as representations of material structure.

One particular draw-back of homology as a metric is the lack of scale in the topological relationships. The size and shape of clusters is of considerable importance in percolation theory .[Grimmett (1999)], yet the homological descriptors do not contain any direct information regarding size or anisotropy of the clusters being counted (see Fig. 1). One way of addressing this issue is to consider the homology of local subsets of the original image by selecting a sub-image via a moving window of varying size. This approach will be termed 'calibrated homology' and will be used in an attempt to improve the correlation between macroscopic material properties and homological structure metrics.

[1] Rough Glossary of Terms:
Homology: a mathematical classification of holes and connected components in a structure
Betti Number, β_i: the number of i-dimensional holes in a structure (β_0 gives the number of connected components)
Relative Homology: the homology of a structure relative to a chosen subspace
Percolation: a measure of connectedness across a structure

In this paper we first convey some of the established methods of linking effective properties to local microstructure. We will then briefly review the relevant aspects of homology before developing the correlations between connectivity and stiffness. Finally, we explore one way of including anisotropy and cluster size of the materials using calibrated homology, and establish how effective it is as a structure metric.

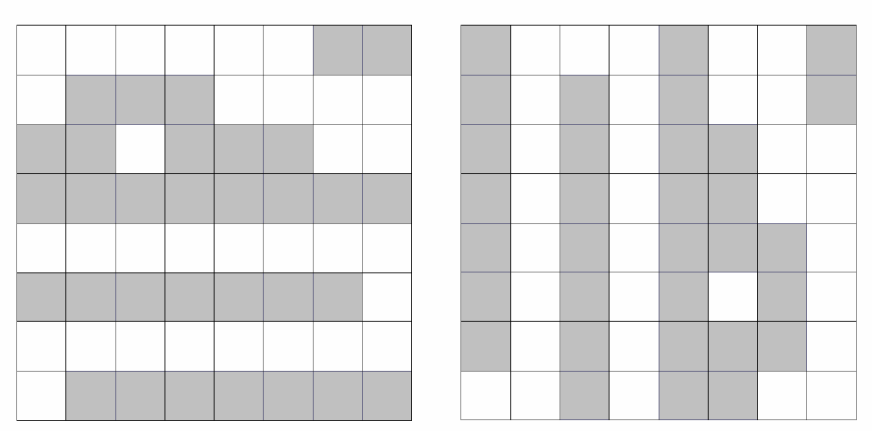

Figure 1: Two plates having the same volume percentage of each material and the same homology, but the plate on the right is stiffer in the vertical direction.

2 Structure Property Linkages

2.1 Homogenization Methods

The application of homogenization theory is a common approach in the determination of effective properties, including heat and mass transfer, mechanical properties, as well as electrical and magnetic properties of heterogenous materials [Fullwood, Niezgoda, Adams and Kalidindi (2010), Milton (2002)]. Homogenization theory depends on the existence of two disparate length scales in the material, the micro-scale which contains the fine structure of the material and the meso-scale where the material is assumed to be a uniform continuum. On the micro-scale the local properties and local response field to a macroscopic force oscillate spatially with a high frequency, whereas on the meso-scale the effective response is assumed to be uniform or slowly varying. The goal of the mathematical theory of homogenization is to replace a differential field equation of the form $\frac{\partial}{\partial x}\left(C\left(\frac{x}{\varepsilon}\right)\frac{\partial u}{\partial x}\right)$, where ε is a very small parameter representing the ratio of micro to meso-scale characteristic

lengths, with the homogenized equation $\frac{\partial}{\partial x}\left(C^* \frac{\partial u}{\partial x}\right)$ where C^* is the homogenized property of interest. This is usually accomplished via an asymptotic expansion in ε of the relevant constitutive laws.

n-point statistics are often used in homogenization theory to capture the local structure of the materials. Two point statistics and higher order statistics have been extensively used to quantify microstructure [Fullwood, Niezgoda, Adams and Kalidindi (2010), Tewari, Gokhale, Spowart and Miracle (2004), Torquato (2002), Zeman and ejnoha (2007)], however it has been repeatedly demonstrated that long range connectivity is not directly captured [Fullwood, Niezgoda, Adams and Kalidindi (2010), Torquato (2002)]. Hence, while homogenization methods work very well for low contrast composites, such as polycrystals, as the contrast is increased, the connectivity of the constituent phases has a significant effect on the effective properties, and homogenization methods fall down. Often, the connectivity is included in a limited manner through the use of higher order homogenization techniques [Kalidindi, Binci, Fullwood and Adams (2006), Kouznetsova, Geers and Brekelmans (2004), Ponte Castañeda (2002)]. Furthermore, some local connectivity information is contained in the 2-point statistics. It is well known that this local connectivity has an effect on longer range connectivity such as the percolation threshold. Hence, while it is not unreasonable to expect a relationship between 2-point statistics and elastic properties for high contrast materials. Nevertheless, for extreme contrasts, such as porous solids, homogenization is a difficult and open research area; metrics that contain long range connectivity information are more likely to provide useful structure-property linkages.

2.2 Percolation Theory

For high contrast materials, percolation theory is often used to predict material behavior. Consider a network of points where adjacent points are either connected, with probability p, or not connected with probability $1-p$; percolation theory seeks to answer whether there is a connected path (or does percolation exist) over a "large" volume. The fraction of connections above which a connected network exists with probability of one, is termed the percolation threshold, p_c. Infinite contrast materials, such as porous solids and foams, must percolate otherwise they will disintegrate and effective stiffness tends to zero. For materials above and near the percolation threshold the elastic stiffness is often given as $C \propto (p-p_c)^T$.[Bergman (1986), Sahimi (1983)]. Percolation is a binary event; either a connected path exists or it does not. In general it is expected that the more connections in the network the higher the stiffness. When p is well above the percolation threshold, the above relationship breaks down. In this case an alternative (and broader) measure of the connectivity such as homology theory would be beneficial.

3 Homology as a Structure Metric

3.1 Definition of Homology

In this section we review some of the definitions relating to homology that lead to the concepts that will be used later in the paper. For the 2D examples considered in this paper we extract two specific homological measures that describe the connectivity of a given phase, comprising the set X, in the simulated material structures. These are the first two Betti numbers, $\beta_0(X)$ and $\beta_1(X)$. Roughly speaking, the number $\beta_0(X)$ represents the number of (disconnected) components of X and the number $\beta_1(X)$ represents the number of independent loops in X. These metrics can be readily calculated using freely available software [CHomP and CAPD (2009)], and the mathematical details presented in the rest of this section are provided for completeness, and can be readily skipped without compromising the main ideas of the paper.

The homology group in dimension n of a cell complex X(in our case X denotes one phase of a microstructure or image), denoted $H_n(X)$, is an algebraic group that contains information about the connectivity of the complex X. If X is a k-dimensional complex, $H_n(X)$ is trivial (empty) for $n \geq k$. In our applications, X is a planar 2-complex, so $H_0(X)$ and $H_1(X)$ will be the only homological groups of interest. $H_n(X)$ can be written as the product of a free group and a torsion group. The Betti number $\beta_n(X)$ is the number of generators for the free group, or, in other words, the number of factors in $H_n(X)$. The torsion group represents twisting, although this group is necessarily trivial for planar complexes. Hence the numbers $\beta_0(X)$ and $\beta_1(X)$ are the only metrics of interest for our 2-D structues. As an example, if X is the union of the shaded squares pictured in Fig. 2, X consists of three connected components, so $\beta_0(X) = 3$, and contains two independent loops, so $\beta_1(X) = 2$. The homology groups are then and .

In order to formally define $H_n(X)$, we must define the chain groups $C_n(X)$, the boundary groups $B_n(X)$, the cycle groups $Z_n(X)$, and the boundary operators $\partial_n : C_n(X) \to C_{n-1}(X)$. For the purpose of illustration, let X denote the cell complex illustrated in Figure 3. Note that X consists of two faces (or 2-cells), seven edges (or 1-cells), and five vertices (or 0-cells). The faces will be assigned the orientation of the forward direction. The orientation of the edges is indicated by the arrows. The orientation of the vertices is positive.

The chain group $C_n(X)$ is the collection of all linear combinations of oriented n-cells in X with integer coefficients, called n-chains. For example, $C_2(X) = \{m_1\sigma_1 + m_2\sigma_2 | m_1, m_2 \in \mathrm{Z}\}$. The boundary operator is a linear operator, $\partial_n : C_n(X) \to C_{n-1}(X)$, that acts on an n-cell $\tau \in \mathbb{Z}$ such that $\partial_n(\tau) = \sum l_i\sigma_i$ where the σ_i are the oriented $n-1$-cells that form the boundary of τ and $l_i = \pm 1$, the sign depending on

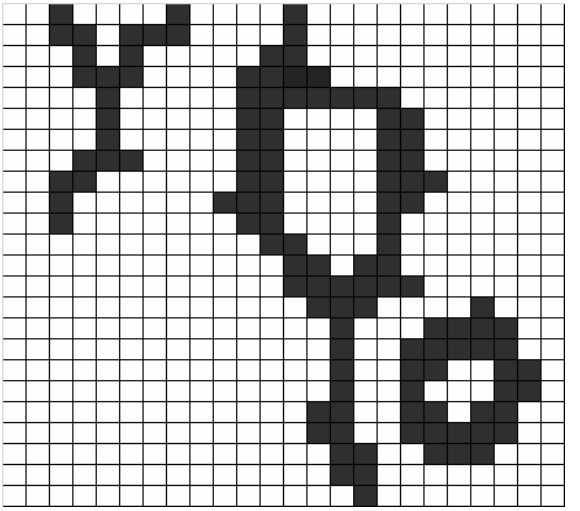

Figure 2: A 2-D structure showing 3 disconnected regions of the black phase (grid-lines are ignored).

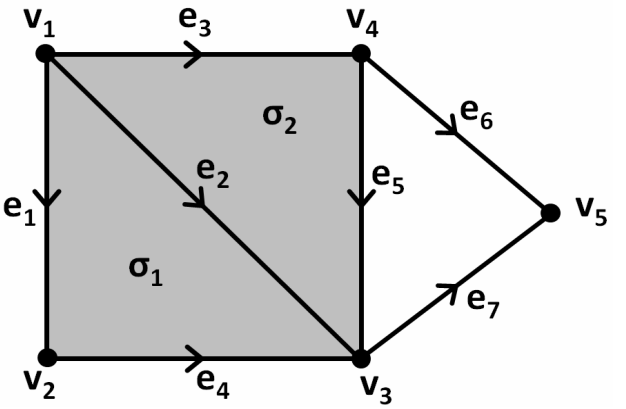

Figure 3: Example of a cell complex, X, with faces denoted by σ, edges by e, and vertices by v.

orientation of σ_i with respect to the orientation of τ. For example, $\partial_2(\sigma_1) = e_1 + e_4 - e_2$, $\partial_1(\sigma_2) = e_2 - e_5 - e_3$, $\partial_1(e_5) = v_3 - v_4$, $\partial_1(e_7) = v_5 - v_3$, $\partial_0(v_i) = 0$. The linearity condition requires that given a chain $\partial_n(c) = m_1\tau_1 + \ldots + m_k\tau_k \in C_n(X)$, the boundary operator satisfies $\partial_n(c) = m_1\partial_n(\tau_1) + \ldots + m_k\partial_n(\tau_k)$. The boundary group $B_n(X)$ is the image of ∂_{n+1}. For example, $-e_5 - e_3 + e_1 + e_4 = \partial_1(\sigma_2 + \sigma_1) \in B_1(X)$,

however $e_3 + e_5 \notin B_1(X)$. The cycle group $Z_n(X)$ is the kernel of ∂_n (i.e., the collection of n-chains $c \in C_n(X)$ such that $\partial_n(c) = 0$). Examples of cycles in $C_1(X)$ include $e_1 + e_4 - e_2$ and $e_5 + e_7 - e_6$. The homology group $H_n(X)$ is the quotient group $Z_n(X)/B_n(X)$. Thus two cycles $Z_n(X)$ in represent the same element $H_n(X)$ in provided that their difference is a boundary of some $n+1$-chain. For example, $e_5 + e_7 - e_6$ and $-e_3 + e_2 + e_7 - e_6$ represent the same element in $H_1(X)$ and $e_1 + e_4 - e_2$ represents the trivial element in $H_1(X)$.

Various other topological properties or invariants such as the Euler characteristic can be calculated directly from the Homology. The Euler characteristic, ψ, is classically defined for polyhedra and relates the number of faces (F), edges (E) and vertices (V) as $\psi = V - E + F$. For all convex polyhedra in n-dimensions $\psi = 2$. The above definition can be generalized for all topological spaces as the alternating sum $\psi = \beta_0 - \beta_1 + \beta_2 - \beta_3 ...$ [Dodson (1996)].

3.2 Relative Homology

In order to connect homological concepts with percolation concepts it is necessary to introduce a further complexity termed relative homology. Percolation theory relates to connectedness between the boundaries of a given domain. If these boundaries are considered as elements in the original structure, relative homology can be used to determine connectedness between them.

The relative homology group in dimension of a cell complex modulo subcomplex A, denoted $H_n(X,A)$, is similar to $H_n(X)$ with the exception that generators in $H_n(X)$ are represented by cycles, or chain complexes with zero boundary, and generators in $H_n(X,A)$ are represented by chain complexes with boundaries that are defined on A. For example, in Fig. 1 suppose that A is a collection of 1-cells forming two borders at the top and bottom of the structure, and X is union of together with the collection of already shaded boxes. Then $H_1(X,A) = \mathbb{Z} \oplus \mathbb{Z} \oplus \mathbb{Z}$. Thus, loosely speaking, the first Betti number for $H_1(X,A)$ is the number of linearly independent loops or independent paths that begin and end in A. If A is a subcomplex of X, the quotient group $C_n(X)/C_n(A)$ is called the group of relative chains of X modulo A, and is denoted $C(X,A)$. In particular, two chains in $C_n(X)$ represent the same chain in $C_n(X,A)$ if and only if the chains differ by a chain in $C_n(A)$. The boundary operator $\partial_n : C_n(X,A) \to C_{n-1}(X,A)$ is defined similarly as before. We define the relative boundary group $B_n(X,A)$ as the image of ∂_{n+1} and the relative cycle group $Z_n(X,A)$ as the kernel of ∂_n. The relative homology group $H_n(X,A)$ is the quotient group $Z_n(X,A)/B_n(X,A)$.

3.3 Conjectured Relationships between Homology and Material Properties

The discussion above indicates, albeit in somewhat vague terms, that a link between 'connectedness' and 'properties' of materials must exist; particularly where there exists a high contrast between the individual properties of composite components. The relationship between connectivity and properties has been well explored using percolation theory. As contrast between material properties increases, percolation scaling laws begin to dominate the composite properties (see, for example, ..[Chen and Schuh (2006)]). One immediate connection between percolation theory and homology is arrived at by considering percolation across an image, X, and utilizing the definitions of relative homology given above.

For a subset of an image, X, (such as that in Fig. 1 or Fig. 2) the number of independent or disconnected percolating paths, n_p, between the top and bottom edges can be determined by adding a connected top border, A, and bottom border, B, and determining:

$$n_p = \beta_1(\mathrm{XA}+\mathrm{B},\mathrm{A}+\mathrm{B}) + \beta_1(\mathrm{X}) - \beta_1(\mathrm{X}+\mathrm{A}) - \beta_1(\mathrm{X}+\mathrm{B}) \tag{1}$$

If the number of paths is not important, one may determine whether percolation has occurred by considering:

$$\beta_1(\mathrm{X}+\mathrm{A}+\mathrm{B},\mathrm{A}+\mathrm{B}) - \beta_1(\mathrm{X}+\mathrm{A}+\mathrm{B}) = \begin{cases} 1 & \text{if percolation has occured} \\ 0 & \text{if percolation has not occured} \end{cases} \tag{2}$$

We note that in percolation theory, on an infinite domain, there is only a single percolating path once the percolation threshold has been passed (i.e. there is only one or zero disconnected paths between the borders).

One of the important measures used in percolation theory is the average cluster size, χ. The average cluster size in a 2D image is given by the total area of the phase of interested, divided by the number of connected components. If V is the area / volume of the domain, and the volume fraction of the phase of interest is p, then:

$$\chi = \frac{V \times p}{\beta_0} \tag{3}$$

This parameter follows a scaling law in the neighborhood of the percolation threshold, p_c [Grimmett (1999)],

$$\chi^f(p) \approx |p - p_c|^{-\gamma} \tag{4}$$

where the superscript, f, is to clarify that only finite clusters are included in the calculation (i.e. not the infinite percolating cluster), the exponent, γ, is the mean

cluster size critical exponent with published value of 2.4 for 2D geometries, and the relation, $\approx$, indicates that

$$\lim_{p \to p_c} \frac{\log\left(\chi^f(p)\right)}{\log\left(|p - p_c|\right)} = -\gamma \tag{5}$$

If the percolating phase is conductive, the conductivity, σ, of the structure in the region of the percolation threshold follows a similar law .[Sahimi (1983)]:

$$\sigma \approx (p - p_c)^t \tag{6}$$

Published values of the conductivity critical exponent, t, are in the region of 1.26 for 2D situations. Hence, by considering the relationships in the previous equations, we expect a scaling law relating β_0 and σ in the region of the percolation threshold, $\sigma \approx \left(\frac{\beta_0}{p}\right)^s$, where $s = t/\gamma$. This relationship is not considered in any detail in this paper, but only mentioned to illustrate potential relationships between homology structure metrics and properties in high-contrast materials.

It should be noted at this point that the scaling law in Eq. (4) relates to all clusters in the structure before the percolation threshold is reached, since they are all finite; however, it applies only to finite clusters once the percolation threshold has been passed. This is not accounted for in the calculation of β_0, and will no doubt affect the anticipated correlation. Furthermore, the percolation theory mentioned above relates to structures of infinite size (in this paper the 2-D domain of a structure is termed a window). Properties of structures of finite size will deviate somewhat from the general theory. For the small windows used for many of the calculations reported below, the percolation threshold will be lower than for an infinite window (see .[Sahimi (1983)]); hence the affects of the small window may need to be compensated for in order to achieve a reasonable correlation between Betti numbers and composite properties.

In terms of the first Betti number, it has been reported in other studies (e.g. [Frary and Schuh (2005)]) that an increasing number of closed loops within clusters affects the volume fraction at which percolation occurs. Hence one may expect a relationship between p_c and β_1. In the subsequent sections various possible relations are explored between homology and physical properties.

4 Simulations

One of the aims of this paper is to ferret out the relationship between homology and global material properties. The initial focus is on global stiffness properties for a two phase material of reasonable contrast laid out on a 2-dimensional plate.

Each plate is composed of a regular n by n array of squares with each square being either material one (M_1) or material two (M_2). The volume percentage of M_1 in the plate is ϕ_1, and similarly the volume percentage of M_2 in the plate is ϕ_2. The Young's modulus of elasticity of M_1 and M_2 can be varied, but M_2 is always stiffer than M_1. After these variables have been defined, a plate is generated by randomly assigning each square to be either M_1 or M_2 such that the volume percentage of M_2 in the plate reaches ϕ_2. The value of n was varied, but intentionally kept small for initial calculation reported below in order to ensure that representative samples from across the space of all possible structures were assessed within a sample space of only hundreds or thousands of trials. After the plate is generated the homological properties of the stiffer phase are computed using the freely available software, CHomP [CHomP and CAPD (2009)]. The input to the CHomP software is a list of coordinates (in two or three dimensions) of the phase of interest. The Betti numbers for the given geometry are output. It should be noted that CHomP not only considers cells that are joined along an edge to be connected, but also cells that are joined at a vertex of the square grid. Clearly the transfer of stress across an edge is much more efficient than transfer across a vertex, and this will clearly affect the strength of any correlation between the homology and overall stiffness.

Next, the Young's modulus of the entire plate is determined. An FEM analysis is performed on the plate using ANSYS ..[(2007)] to determine the effective Young's modulus in the vertical direction. The bottom nodes are constrained and the top nodes are displaced a certain distance to allow for elastic deformation in the plate. Figure 4 demonstrates an example geometry output from ANSYS.

The Matlab [(2006)] computation environment was used to generate the material geometries, run the CHomP and ANSYS codes, and analyze and visualize the results.

5 Correlations between Homology and Stiffness at Different Volume Fractions

5.1 Betti Numbers Related to Stiffness and a Single Volume Fraction

Figures 5 and 6 present two graphs relating homology to the stiffness of the plate. For this simulation n=16 and each of these plates is generated by randomly assigning each element to be M_1 or M_2 and $\phi_2 = 0.5$. The modulus of elasticity of M_1 is 10^8Pa and the modulus of elasticity of M_2 is 700×10^8Pa. Figure 5 correlates the β_0 number of a plate to the stiffness of the plate. Figure 5 correlates the number of a plate to the stiffness of the plate. There are 250 sample points in each graph. The least square R^2 value is given to describe how strong of a correlation is achieved. The closer is to one, the better the correlation is.

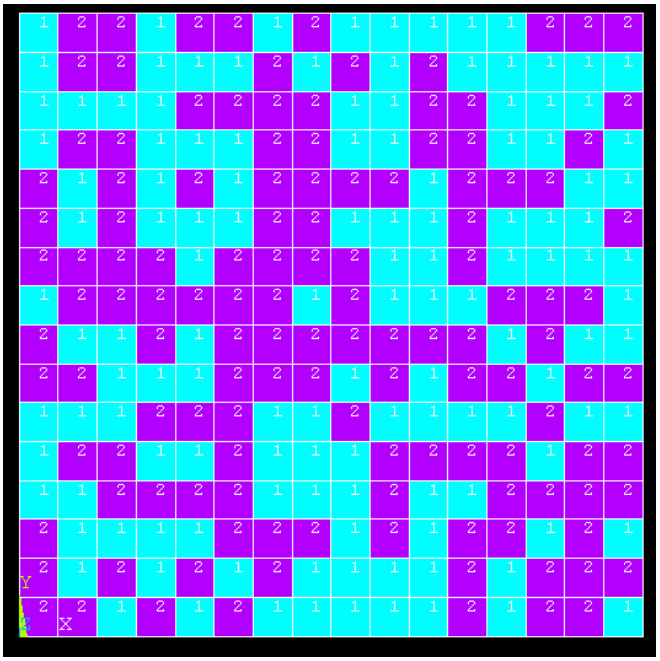

Figure 4: An $n = 16$, $\phi_2 = 0.5$ heterogeneous plate in ANSYS.

Figures 5 and 6 demonstrate that there is a correlation between the phase homology and the plate stiffness. The distribution of data points for any given Betti number is a normal distribution about the trend line of the graph. While there is a significant amount of scatter in the data, the general relationship between the stiffness, E, and β_0 follows the relationship predicted by Eqs. (3), (4) and (6) (as can be easily derived from a log-scale graph of Fig 5):

$$E = 9.06 \times 10^9 \times \beta_0^{-0.12899} \tag{7}$$

To intuitively understand why these correlations exist, two plates are shown in Fig. 7. M_1 is the white material and M_2 is the darker material. The plate on the right has $\beta_0 = 11$ and $\beta_1 = 0$ while the plate on the left has $\beta_0 = 1$ and $\beta_1 = 11$. The disconnected nature of the stiff phase in the right figure (corresponding to high β_0) means that stress is not efficiently transferred across the plate, resulting in low stiffness. Similarly, in the left figure, the low value of β_0, and the high value of β_1 indicates good connectivity (and stress transfer) for low volume fractions of the stiff phase (the areas of the softer phase being surrounded by stiff material). Hence, for this type of geometry, it is clear that stiffness is likely to increase with decreasing

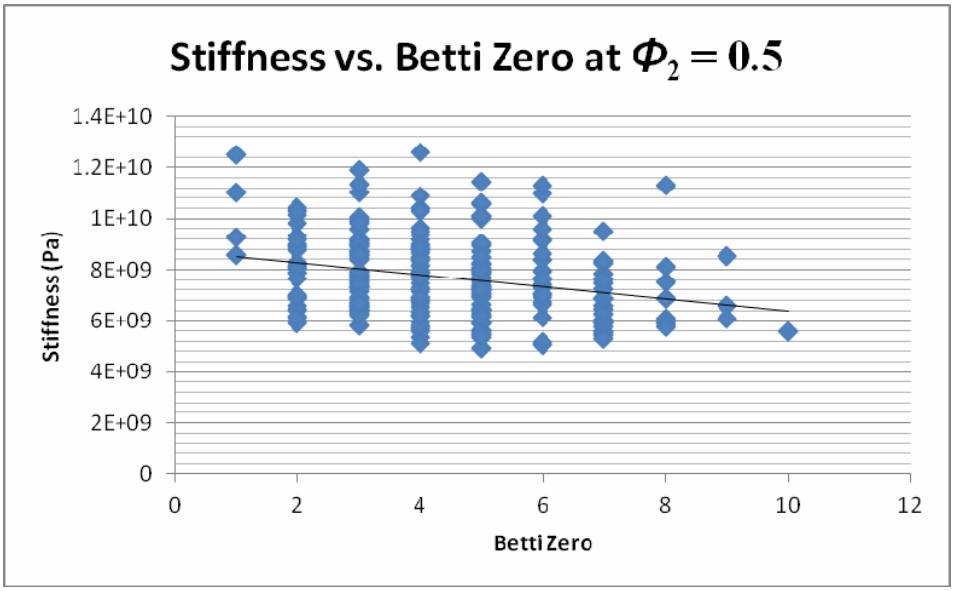

Figure 5: Stiffness vs. (β_0) for 250 structures with volume fraction of each phase = 0.5. The R-squared value for the trend line is $R^2 = 0.07171$

β_0 and with increasing β_1.

The samples reported above were created by randomly assigning phases. The potential property extrema achievable in non-random arrangements were investigated by considering special structures.

Figure 8 illustrates the stiffness properties of four special structures in relation to the random ones previously generated. The data series 1 is the same data that is given in Fig. 5. The other four data points are four specifically designed plates. Each plate has $\beta_0 = 4$ and $\beta_1 = 0$. The plate with the largest stiffness (as measured in the vertical direction) is a vertical arrangement of 4 columns. Similarly, the point with the lowest stiffness is a horizontal arrangement of M_1 and M_2. The second highest stiffness shown on the figure is a plate with M_2 in an arrangement that is largely vertical but with a few idiosyncrasies. The plate with the second smallest stiffness is made from four large, tight clusters of M_2.

Clearly the Betti zero number of the special structures does not accurately reflect their extreme nature. On the other hand, the number of percolating paths for these structures is clearly special. Hence, some measure of local homology – relating to the size / shape of clusters in a sample – may give better correlation in terms of predicting physical properties.

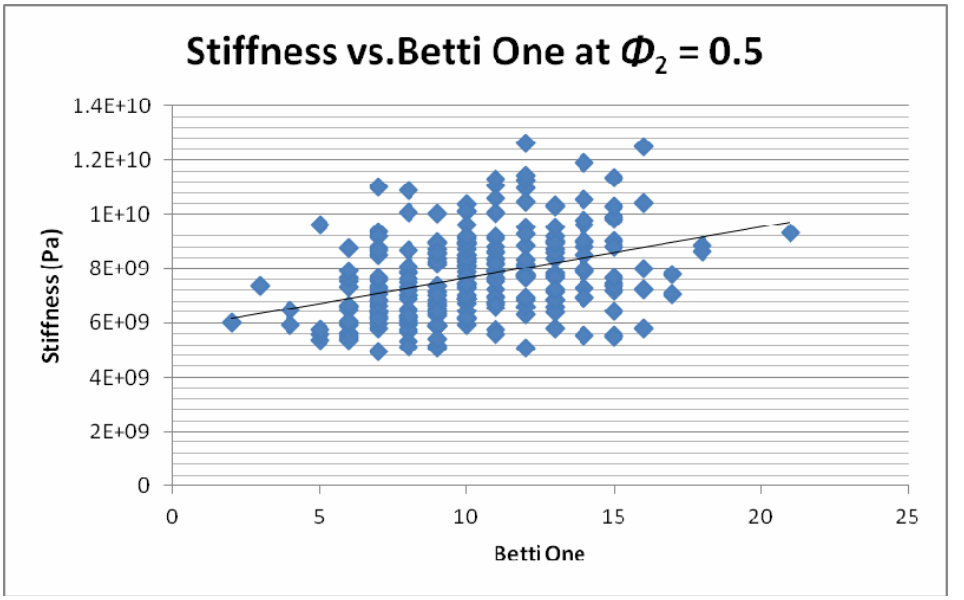

Figure 6: Stiffness vs. (β_1) for 250 structures with volume fraction of each phase = 0.5. The R-squared value for the trend line is $R^2 = 0.13236$

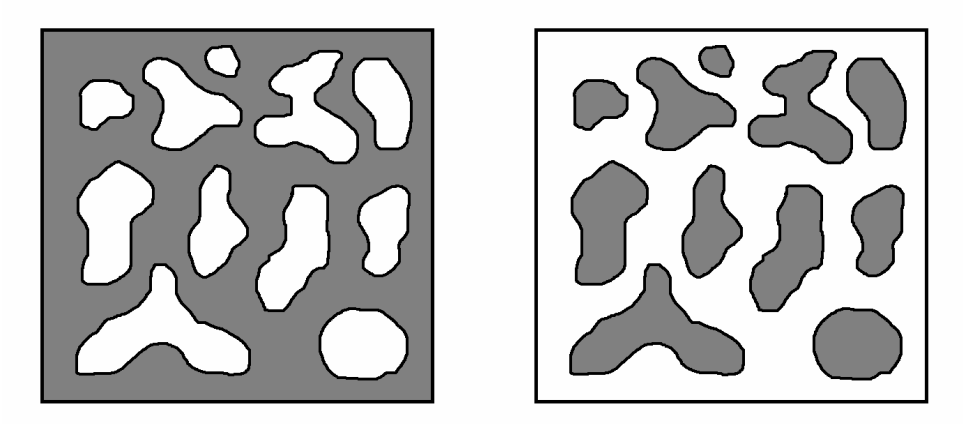

Figure 7: Two plates with the same ϕ_2 but different homology.

5.2 Effects on Homology due to Volume Fraction

Now we see how homology and stiffness are affected by varying the volume fraction of M_1 and M_2. The results of several simulations are given below. Figure 9

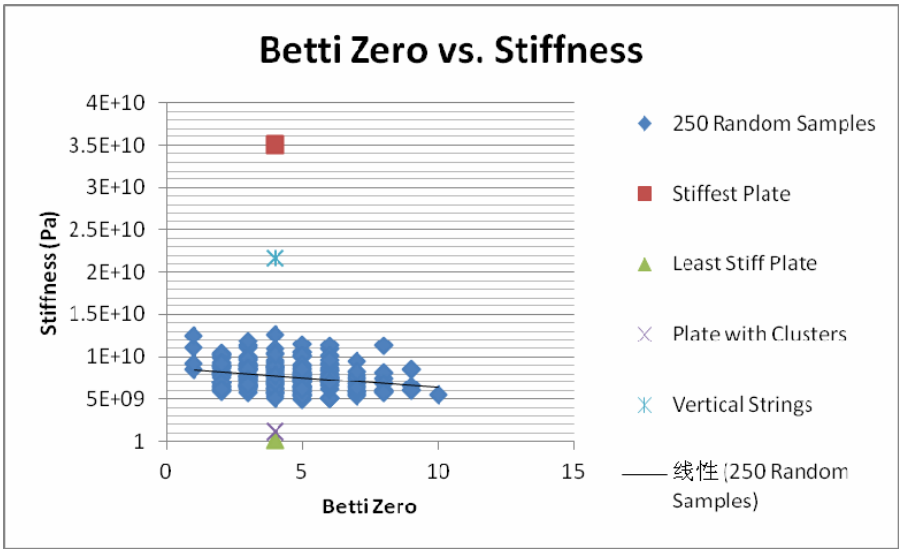

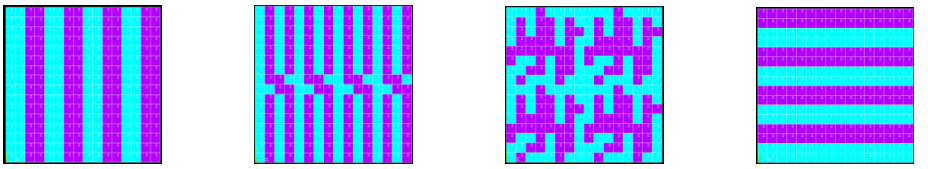

Stiffest Plate Vertical Strings Clusters Least Stiff

Figure 8: The graph above plots the data for four plates with the same homology. The data for the plates with the largest and smallest stiffness is plotted along with the data for two other plates with intermediary stiffnesses.

relates the stiffness in the vertical direction to β_0 for 250 samples randomly generated as before, where the volume fraction is $\phi_2 = 0.25$. Figure 10 relates the stiffness to β_1 for 250 random samples where the volume fraction is $\phi_2 = 0.75$.

These improved correlations shown in these two graphs highlight the fact that different homology descriptors provide better structure metrics at different volume fractions – at least for the finite samples used in this study. When $\phi_2 = 0.25$ for a random plate, the stiffness is best related to β_0, but at $\phi_2 = 0.75$ the stiffness is best related to β_1. This is illustrated by the figures in Table 1. This trend is partially due to the limited range of the Betti numbers at extremes of volume fraction in the small samples. For example, when $\phi_2 = 0.75$ there were only two different outcomes for β_0 in the simulations that were run. Figure 11 shows data for the stiffness and β_0

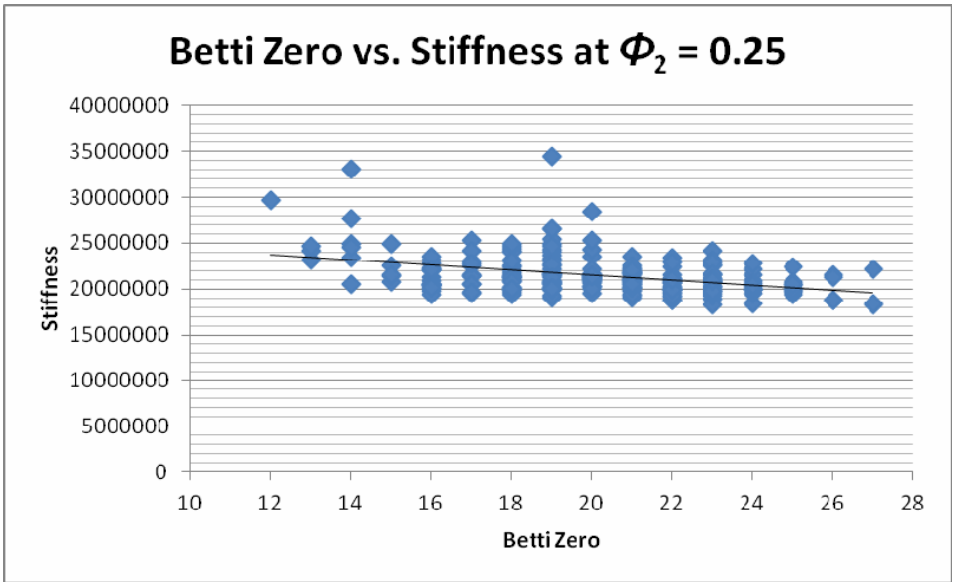

Figure 9: β_0 vs. stiffness for 250 structures with 0.25 volume fraction of M_2. The R-squared value for the trend line is $R^2 = 0.13236$

for $\phi_2 = 0.75$. The narrow domain of Betti numbers doesn't provide an adequate sample space to allow for a strong correlation.

Table 1: The table below gives the R-squared values correlating trend lines between Betti zero and the stiffness of a plate in the vertical direction at different volume fractions.

ϕ_2	R_0^2
0.25	0.15679
0.50	0.07171
0.75	0.00310

For small volume fractions of the correlation is better using β_0 but for large volume fractions the correlation improves by using β_1. At smaller volume fractions β_0 tends to be larger and β_1 tends to be smaller. In general, the roles are then reversed as the volume fraction increases. When the domain of the Betti number of choice is larger there is a greater likelihood that a strong correlation will occur. We performed an analysis to relate to ϕ_2 both β_0 and β_1.

It should also be noted that from the discussion around Eqs. (3), (4) and (6), the

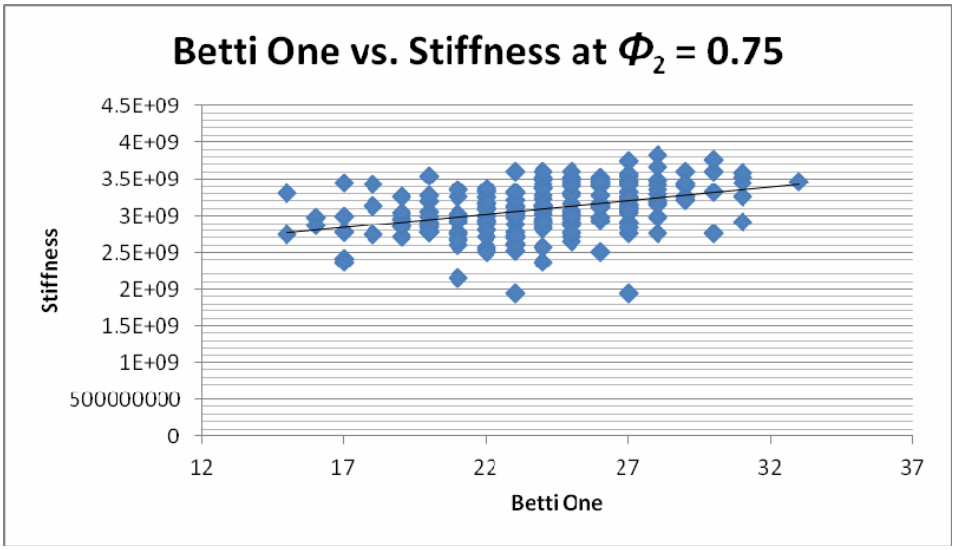

Figure 10: β_1 vs. stiffness for 250 structures with 0.75 volume fraction of M_2. $R^2 = 0.14288$

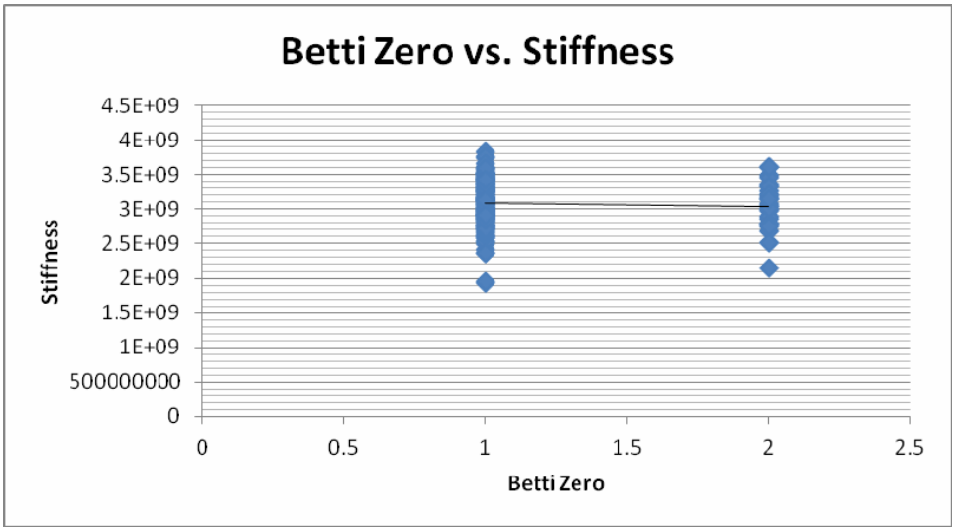

Figure 11: β_0 vs. stiffness for 250 structures with 75 volume fraction of M_2. $R^2 = 0.00310$

correlation with Betti zero is expected to improve below the percolation threshold,

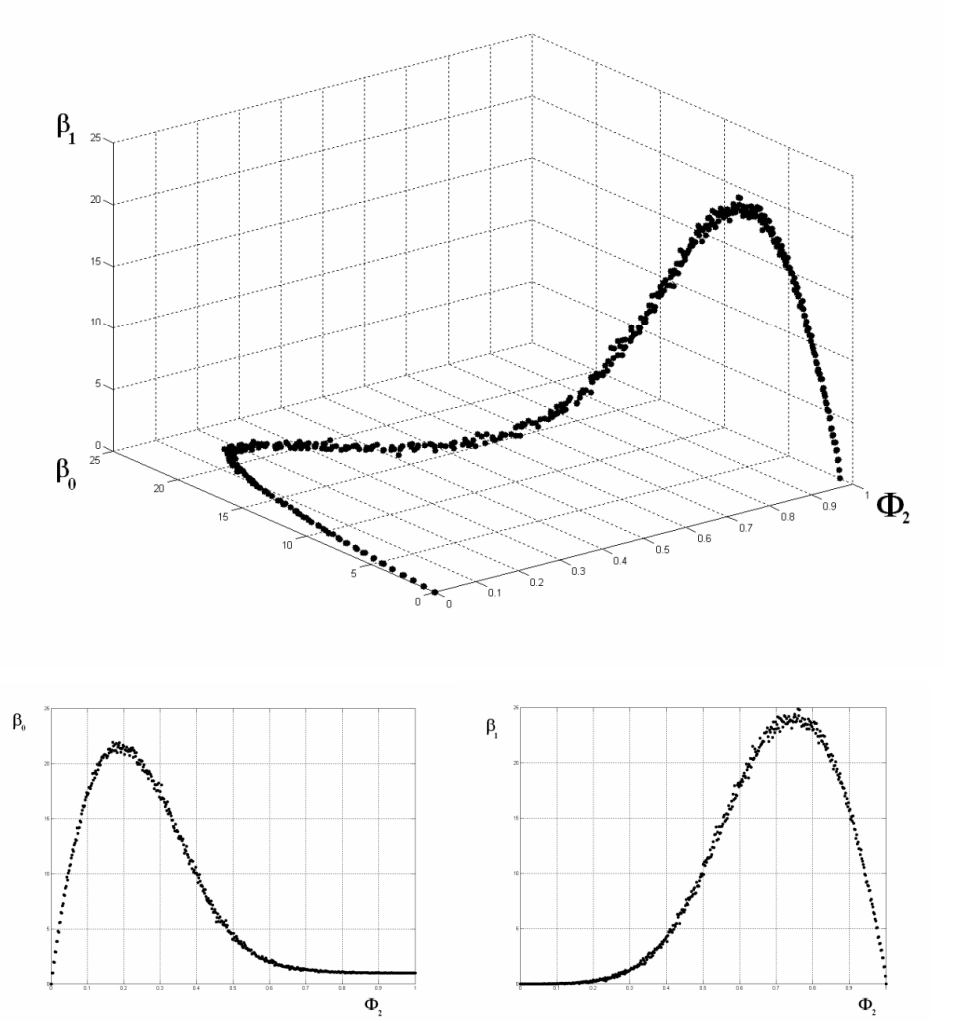

Figure 12: The graph on the bottom left relates ϕ_2 to β_0 and the graph on the bottom right relates ϕ_2 to β_1 both for randomly generated $n = 16$ plates. These are views from the three dimensional plot above.

Table 2: The table below gives the R-squared values correlating trend lines between Betti one and the stiffness of a plate in the vertical direction at different volume fractions.

ϕ_2	R_1^2
0.25	0.01490
0.50	0.13236
0.75	0.14288

which is approximately 0.41 for site percolation on an infinite window of the lattice in question (note that this is different from published values of 0.59 for site percolation on a square lattice, due to differing definitions of connectivity. In standard lattices, sites that contact across a vertex rather than an edge are not considered to be connected; in the CHomP definition, they are).

6 Further Insights

6.1 Calibrated Homology

The images in Fig. 1 highlight the potential for anisotropy to affect the properties of structures. The Betti metrics do not contain information regarding directionality of the connectedness in a structure. One method of determining such directionality is to consider homology on particular subsets of a structure by investigating connectivity across sub-windows of varying shapes and sizes. We define "calibrated homology" as the homology of a local area of the original plate. Many options exist for varying the size and shape of sub-windows, and thereby extracting more information regarding the typical cluster size and shape. In this section we use calibrated homology to find the maximum cluster height within a structure. In Fig. 1, for example, the plate on the left has a maximum cluster height of 3, and the plate on the right has a maximum cluster height of 8.

Cluster height is determined by taking sample windows whose widths are equivalent to the width of the plate but whose heights vary. For an n=16 plate we start with a window that is 16 elements long and 1 element high. We place this window at all 16 possible positions on the plate and use Eq. (2) to determine whether or not the sample within the window has a percolating path from top to bottom. We then increase the window size until the window height is larger than all clusters contained within it. We defined the maximum cluster height as the threshold at which percolation occurs.

In the following simulations we find the maximum cluster height of phase M_2 for 250 structures, and correlate it to the vertical stiffness. Again, each plate is gener-

ated randomly with n=16 and $\phi_2 = 0.5$.

Figure 14 illustrates a typical set of results relating the maximum cluster height of a plate to its stiffness. While the graph highlights a definite correlation between the two parameters, the strength of the correlation (given by R^2) is of the same order as that given by the Betti numbers alone (and reported above). Nevertheless, this small foray into calibrated homology indicates that the choice of a more suitable local window size / shape may lead to better correlations between the homology metrics and material properties.

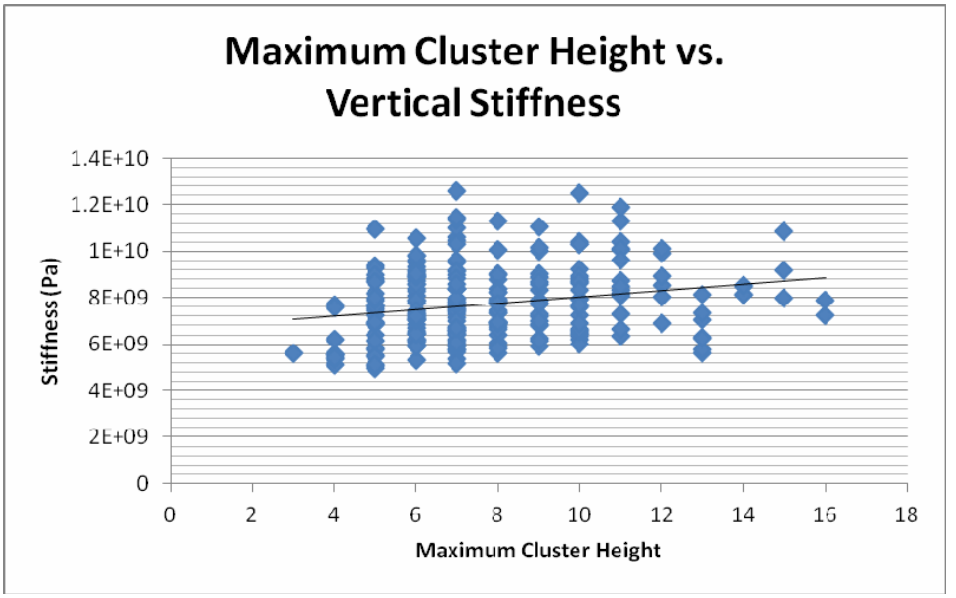

Figure 13: Maximum Cluster Height, h_c, vs. Stiffness. $R^2 = 0.0501$

6.2 Effects of Higher Contrast between and

One obvious question regarding the results presented above involves the impact that the contrast between properties of the individual phases has on the correlations. As contrast increases, the role that connectivity plays in determining the resulting properties would be expected to increase. For the previous simulations, the modulus of elasticity of was 700 times that of M_1. Here we look at higher contrasts. For this analysis we still leave $n = 16$ and $\phi_2 = 0.5$.

The results are given in Table 3, and indicate that for the particular properties of interest in this study, and for the particular definition of connectedness, contrasts

in properties above 700 do not result in a significantly higher correlation between stiffness and connectivity as measured by the Betti numbers.

Table 3: R-squared values for correlations between stiffness and Betti numbers (the subscript on R corresponding to the 0^{th} or 1^{st} number) for phases of varying contrast

Contrast	R_0^2	R_1^2
700	0.07171	0.13236
7,000	0.06501	0.13802
70,000	0.05517	0.13711
700,000	0.03422	0.15110

6.3 Effects of a Larger Window Size (n)

The effects of window size on the main results of the paper were also investigated. Again, the modulus of elasticity of is taken to be 700 times that of the modulus of M_1 and $\phi_2 = 0.5$. The results are given in Table 4, and indicate that the correlation between Betti number and stiffness drops off sharply as the window size increases for the random structures presented in this paper. One explanation for this may be that for large structures, above the percolation threshold, the properties are dominated by the single infinite cluster, and only weakly dependent upon the other finite clusters (which potentially dominate the Betti number values). This may also be indicative of the fact that the structure is becoming homogeneous at the larger window size - the individually generated samples are statistically almost identical at the larger size. The result indicates that the correlation value can be used to help determine suitable dimensions for representative volume elements (RVE) – domains over which the structure is statistically homogeneous. This will be discussed in a separate paper. Furthermore, non-random structures will also be considered.

Table 4: R-squared values for correlations between stiffness and Betti numbers (the subscript on R corresponding to the 0^{th} or 1^{st} number) for windows of varying size

n	R_0^2	R_1^2
16	0.07171	0.13236
32	0.00981	0.15411
64	0.00207	0.13668
128	0.00002	0.04869

7 Conclusions

This paper presents an initial investigation into structure metrics provided by homology, and their relation to material properties. Some relationships between percolation theory and homology have been noted for the first time (to our knowledge). Furthermore, from the calculations reported above, there is clearly a correlation between connectivity as measured by Betti numbers, and stiffness of resulting structures, for high contrast composites. However, the correlation is perhaps not as strong as expected, and future investigations will consider electrical conductivity of structures, which is more typically associated with percolation type property relations (and hence, connectedness metrics). Non-random structures will also be considers, along with an investigation into the definition of RVEs via homology metrics.

Acknowledgement: The authors wish to acknowledge the Computational Homology Project at Rutgers University. D Gerrard also acknowledges funding from Brigham Young University College of Physical and Mathematical Science and Drexel University DREAM Research Experience for Undergraduates.

References

(2007): *ANSYS 11.0*, ANSYS, Inc.

(2006): *Matlab*, The Mathworks, Inc.

Adams, M. (Submitted): Correlation between effective stiffness and homological connectivity, *Journal of Elasticity*,

Arbabi, S., Sahimi, M. (1993): Mechanics of disordered solids. I. Percolation on elastic networks with central forces, *Physical Review B*, 47, 2, 695

Beran, M. J., Mason, T. A., Adams, B. L., Olsen, T. (1996): Bounding elastic constants of an orthotropic polycrystal using measurements of the microstructure, *Journal of the Mechanics and Physics of Solids*, 44, 9, 1543-1563

Bergman, D. J. (1986): Elastic moduli near percolation in a two-dimensional random network of rigid and nonrigid bonds, *Physical Review B*, 33, 3, 2013

Chen, Y., Schuh, C. A. (2006): Diffusion on grain boundary networks: Percolation theory and effective medium approximations, *Acta Materialia*, 54, 18, 4709-4720

CHomP, R. U., CAPD, N. L. U. P. (2009): *Computational Homology Project, CHomP*,

Curtin, W. A., Miller, R. E. (2003): Atomistic/continuum coupling in computational materials science, *Modelling and Simulation in Materials Science and Engineering*, 11, R33-R68

Dodson, C. (1996): *User's guide to algebraic topology*, Kluwer Academic,

Frary, M., Schuh, C. A. (2005): Grain boundary networks: Scaling laws, preferred cluster structure, and their implications for grain boundary engineering, *Acta Materialia*, 53, 16, 4323-4335

Fullwood, D., Niezgoda, S., Adams, B., Kalidindi, S. (2010): Microstructure Sensitive Design for Performance Optimization, *Progress in Materials Science*, 55, 477-562

Gameiro, M., Mischaikow, K., Wanner, T. (2005): Evolution of pattern complexity in the Cahn-Hilliard theory of phase separation, *Acta Materialia*, 53, 3, 693-704

Ghrist, R., Muhammad, A. (2005): *Coverage, hole-detection in sensor networks via homology*, IEEE Press,

Goubault, E., Jensen, T. (1992): *Homology of higher dimensional automata*, 254-268

Grimmett, G. (1999): *Percolation. 2nd ed.*, Springer, 321,

Ju, J., Chen, T. (1994): Micromechanics and effective moduli of elastic composites containing randomly dispersed ellipsoidal inhomogeneities, *Acta Mechanica*, 103, 1, 103-121

Kalidindi, S. R., Binci, M., Fullwood, D., Adams, B. L. (2006): Elastic properties closures using second-order homogenization theories: Case studies in composites of two isotropic constituents, *Acta Materialia*, 54, 11, 3117-3126

Kantor, Y., Webman, I. (1984): Elastic Properties of Random Percolating Systems, *Physical Review Letters*, 52, 21, 1891

Kouznetsova, V. G., Geers, M. G. D., Brekelmans, W. A. M. (2004): Multi-scale second-order computational homogenization of multi-phase materials: a nested finite element solution strategy, *Computer Methods in Applied Mechanics and Engineering*, 193, 48-51, 5525-5550

Kumar, H., Briant, C. L., Curtin, W. A. (2006): Using microstructure reconstruction to model mechanical behavior in complex microstructures, *Mechanics of Materials*, 38, 818-832

Mecke, K. R. (1996): Morphological characterization of patterns in reaction-diffusion systems, *Physical Review E*, 53, 5, 4794

Mecke, K. R., Sofonea, V. (1997): Morphology of spinodal decomposition, *Physical Review E*, 56, 4, R3761

Mendoza, R., Thornton, K., Savin, I., Voorhees, P. W. (2006): The evolution of interfacial topology during coarsening, *Acta Materialia*, 54, 3, 743-750

Mezey, P. G. (1985): Group theory of electrostatic potentials: A tool for quantum

chemical drug design, *International Journal of Quantum Chemistry*, 28, S12, 113-122

Milton, G. W. (2002): *The Theory of Composites* Cambridge University Press

Phillips, R. (2001): *Crystals, defects and microstructures : modeling across scales*, Cambridge University Press,

Ponte Castañeda, P. (2002): Second-order homogenization estimates for nonlinear composites incorporating field fluctuations: II–applications, *Journal of the Mechanics and Physics of Solids*, 50, 4, 759-782

Roberts, A. P., Garboczi, E. J. (2002): Elastic properties of model random three-dimensional open-cell solids, *Journal of the Mechanics and Physics of Solids*, 50, 1, 33-55

Rudd, R. E., Broughton, J. Q. (2000): Concurrent Coupling of Length Scales in Solid State Systems, *physica status solidi (b)*, 217, 1, 251-291

Sahimi, M. (1983): Critical Exponent of Percolation Conductivity by Finite-Size Scaling, *Journal of Physics C: Solid State Physics*, 16, L521-527

Sankaran, S., Zabaras, N. (2006): A maximum entropy approach for property prediction of random microstructures, *Acta Materialia*, 54, 8, 2265-2276

Steele, J. H. (1972): *Application of topological concepts in stereology*, American Society for Testing and Materials, 39-58

Tewari, A., Gokhale, A. M., Spowart, J. E., Miracle, D. B. (2004): Quantitative characterization of spatial clustering in three-dimensional microstructures using two-point correlation functions, *Acta Materialia*, 52, 2, 307-319

Torquato, S. (2002): *Random heterogeneous materials : microstructure and macroscopic properties*, Springer

Wanner, T., Fuller Jr, E. R., Saylor, D. M. (2010): Homology metrics for microstructure response fields in polycrystals, *Acta Materialia*, 58, 1, 102-110

Zbib, H. M., Diaz de la Rubia, T. (2002): A multiscale model of plasticity, *International Journal of Plasticity*, 18, 9, 1133-1163

Zeman, J., ejnoha, M. (2007): From random microstructures to representative volume elements, *Modelling and Simulation in Materials Science and Engineering*, 15, S325-S335